Heliyon 9 (2023) e19985

Contents lists available at ScienceDirect

Heliyon

journal homepage: www.cell.com/heliyon

Enhancing isolation performance of tilted Beam MIMO antenna for short-range millimeter wave applications

Wahaj Abbas Awan [a], Esraa Mousa Ali [b], Mohammed S. Alzaidi [c], Dalia H. Elkamchouchi [d], Fahad N. Alsunaydih [e], Fahd Alsaleem [e], Khaled Alhassoon [e,*]

[a] Department of Information and Communication Engineering, Chungbuk National University, Cheongju 28644, South Korea
[b] Faculty of Aviation Sciences, Amman Arab University, Amman 11953, Jordan
[c] Department of Electrical Engineering, College of Engineering, Taif University, P.O. Box 11099, Taif 21944, Saudi Arabia
[d] Department of Information Technology, College of Computer and Information Sciences, Princess Nourah bint Abdulrahman University, P.O. Box 84428, Riyadh 11671, Saudi Arabia
[e] Department of Electrical Engineering, College of Engineering, Qassim University, Unaizah 56452, Saudi Arabia

ARTICLE INFO

Keywords:
Compact electronics
IoT
Isolation improvement
Millimeter wave
MIMO antenna

ABSTRACT

The research paper discusses the detailed designing of a compact, simple, and low-profile antenna that provides several desirable features. The antenna is engineered by using a substrate material called Roger 6002, and its dimensions are 12 mm × 6 mm × 1.52 mm. The single antenna element achieves a wideband frequency coverage of 24–30.2 GHz and a high gain of 9 dBi. To enhance the antenna's capabilities, a two-port multiple-input multiple-output (MIMO) configuration is employed by adding a second antenna element orthogonal to the first one. Although the operational band remains the same, the isolation between the two elements is found to be unsatisfactory. A C-shaped decoupling structure is established to address this issue, which effectively improves the isolation. Including the parasitic patch enhances the isolation from −18 dB to −29 dB. An antenna hardware sample is built and tested to validate the recommended work, and the outcomes are compared to the predicted results obtained from the software. The experimental and simulated data exhibit close agreement, confirming the accuracy of the design. Additionally, this outstanding performance in bandwidth and isolation compares with existing literature, presented in the form of a table. Various MIMO parameters are also examined, and it is found that they fall within acceptable ranges. The antenna demonstrates an Envelope Correlation Coefficient (ECC) of approximately 0.005 and a Diversity Gain (DG) of around 9.99 dB. The recommended antenna design is highly suitable for future miniature devices used in Internet of Things (IoT) applications.

* Corresponding author.
E-mail addresses: wahajabbasawan@chungbuk.ac.kr (W.A. Awan), esraa_ali@aau.edu.jo (E.M. Ali), m.alzaidi@tu.edu.sa (M.S. Alzaidi), dhelkamchouchi@pnu.edu.sa (D.H. Elkamchouchi), f.alsunaydih@qu.edu.sa (F.N. Alsunaydih), f.alsaleem@qu.edu.sa (F. Alsaleem), K.hassoon@qu.edu.sa (K. Alhassoon).

https://doi.org/10.1016/j.heliyon.2023.e19985
Received 12 July 2023; Received in revised form 1 September 2023; Accepted 7 September 2023
Available online 9 September 2023

1. Introduction

Current research on mobile Internet of Things (IoT) connections depends extensively on an immediate rise in data rates. To increase data rates and fulfill the beneficial needs of LTE (long-term evolution) and the fifth generation, a lot of work has been done [1–3]. IoT gadgets, on the other hand, want a larger data rate. The Federal Communication Commission (FCC) has now officially reserved 5G bands at lower frequencies (sub-6 GHz) and higher frequencies (mm-wave band), which are utilized for 5G mobile communication to increase data throughput [4,5]. In MIMO antenna systems, the data rates are further enhanced by the use of a larger number of antennas [6].

The IoT communication scenario given in Fig. 1 illustrates that a high data rate is required to cover a large coverage area [7]. The evidence of the requirement for high data rates for future IoT applications in the 6G system is the current 4G and 5G communication devices [8]. A high data rate is required for mobile communication for personal interaction as well as interaction between various nodes. In future IoT systems, human interaction will be possible with the body for health care purposes as well as with other bodies present in the environment. This concept is the idea of smart cities, where one will communicate with nearby vehicles, IoT devices, etc. [9–11].

The above brief discussion shows that a high data rate is a keen requirement for future 5G and 6G devices [12]. For this consideration, as an antenna is a key component of any communication device, the requirement for an antenna is also revised [13]. An antenna with a wideband and high gain is considered to get an efficient data rate, but for IoT devices, the compact size, low profile, and simplified structure are also important. The abovementioned features are exploited in literature, and many papers are reported [14–16].

Fig. 1 expresses the usage of millimeter-wave antennas in future communication systems. The importance of antennas can be seen in satellite communication, vehicle-to-vehicle communication, vehicle-to-any-object communication, smartphones, and IoT devices. Mobile phone-based millimeter wave antennas are given in Refs. [17,18] for broadband applications. In the case of a MIMO antenna system, isolation is an important parameter, which can be improved in multiple ways. In Ref. [19], the isolation of the antenna is enhanced by using a defective ground structure (DGS), while in Ref. [20], a slotted stub is loaded to improve the isolation between MIMO elements. There are also many other efficient techniques to boost the isolation of MIMO antennas, which include the introduction of metamaterials like parasitic elements, EBGs, or metasurfaces [21].

Fig. 2 represents the PCB circuit model consisting of the antenna and other circuit components. The circuit is arranged and engineered for IoT applications. It can be seen from the figure that IoT devices are used for smart homes, smart vehicles, Wi-Fi connections, and smartphones and watches [22]. It can also be observed that these devices are also used in the monitoring of agricultural land and health centers. Moreover, IoT also has applications in satellite communication systems [23].

In the literature, most of the work is conducted on the isolation improvement of MIMO antennas, but they have some limitations: complexity, large size, low value of isolation, narrow band, or low gain. Some of this work is briefly explained in this section. A dielectric resonator antenna (DRA) and its MIMO configuration are given in Ref. [24], where metallic strips are loaded to refine the isolation of the antenna. Although the antenna has a compact size of 20 mm by 20 mm, it operates in a narrow band of 27.5–28.35 GHz. A wideband antenna offering 27–32 GHz with improved isolation of −38 dB by loading meta-surface. The antenna has a wideband and low isolation but a complex geometrical structure and a size of 85 mm × 21 mm [25].

A high-isolation antenna loaded with parasitic patches is reported in Ref. [26]. The antenna is 30 mm × 35 mm overall and has a 1 GHz operating bandwidth. The antenna is small, has a simplistic shape, and operates in a narrow band; in contrast, a millimeter-wave antenna provides a wider bandwidth [27]. presents a wideband antenna with enhanced isolation achieved by loading the meta-surface. Wideband, high gain, and minimal mutual coupling are all features of the described design; however, it has a large size and complex shape [28]. provides a dual-port DRA antenna for wide-band 5G applications. The antenna has a bandwidth of 26–30.5 GHz and a low isolation of −41 dB. Although the antenna is small, its mathematical arrangement is intricate.

A wideband antenna offering 26–31 GHz bandwidth is given in Ref. [29]. The antenna isolation is improved to −21 dB by placing parasitic elements between MIMO elements. The value of isolation is acceptable but larger than other antennas given in the literature. A small antenna with measurements of 26 mm by 14.5 mm offers a bandwidth of 27–29 GHz. It is noticed that from −19 dB to −21 dB by placing a meta-surface, the mutual coupling is reduced. Although antennas have good values in bandwidth and isolation, they are lower than in other literature. On the other hand, the overall design is complex because of the meta-surface. Isolation-improved MIMO antennas based on meta-surface are given in Refs. [30,31]. The antenna has measurements of 20 mm by 40 mm with an isolation of

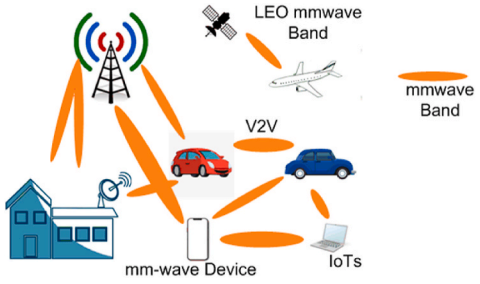

Fig. 1. Representation of mm-wave device connection in IoT environment.

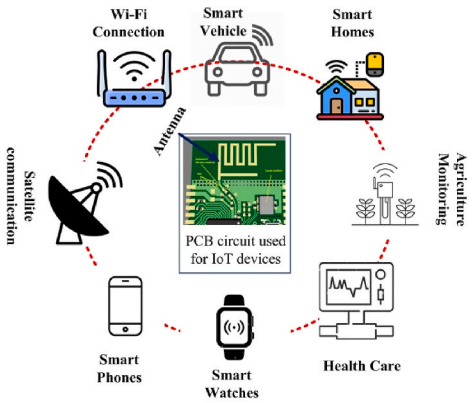

Fig. 2. Application of IoT devices loaded with the antenna.

−28 dB.

This is clear from the above discussion: there is still a need to develop antennas with compact dimensions, straightforward geometry, strong gain, wide bandwidth, and minimal isolation. In recommended work, a two-port MIMO antenna for the 5G communication system was developed with the following uniqueness.

- *Compact size and simple as well as novel geometry.*
- *The simple and novel shape of a parasitic patch.*
- *Wide operational bandwidth and high gain.*
- *Low mutual coupling.*
- *Suitable for future IoT devices.*

Moreover, this paper explains the single antenna, simulated outcomes, and measurement results. The MIMO antenna whether having parasitic elements or not is also explained. The antenna results are compared with the literature to show the uniqueness of this work in the form of a table. In the end, the references as well as conclusion is given.

2. Design and results of unit element

2.1. Antenna design methodology

Fig. 3(a–b) depicts the preferred antenna's design. The antenna is intended to be mounted on the Roger 6002 substrate material, which has a loss tangent of 0.0012 and a relative permittivity of 2.94. The suggested design has a size of $S_X \times S_Y \times t = 12$ mm $\times$ 6 mm $\times$ 1.52 mm and contains a simple microstrip feedline loaded with two rectangular and one elliptical stub. The center of the elliptical stub is etched by a circular slot having a radius of R_2. The stub is loaded, and a slot is etched to strengthen the impedance and bandwidth of the antenna. The optimized parameter of the antenna is given below:

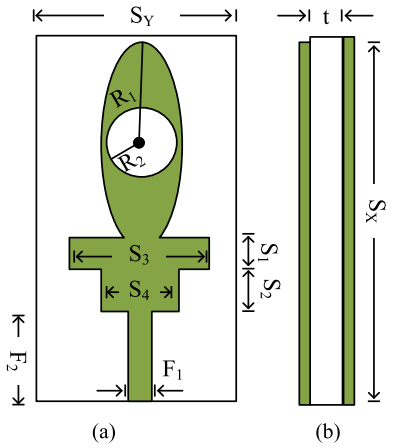

Fig. 3. The shape of the suggested antenna (a) top view (b) side view.

$S_X = 12$; $S_Y = 6$; $t = 1.52$; $S_1 = 1$; $S_2 = 1$; $S_3 = 4$; $S_4 = 2$; $F_1 = 0.5$; $F_2 = 2$; $R_1 = 4$; $R_2 = 1.5$. (All units are in mm)

Following several design phases, the proposed antenna's final geometry was achieved. The rectangular patch antenna featuring a microstrip feedline was developed for 27 GHz in the initial phase [32]. The antenna provides a 26.5–27.5 GHz impedance bandwidth. In the second stage, one more stub is introduced with a rectangular shape to improve the bandwidth as well as the $|S_{11}|$ The antenna after this stage offers a wideband of 26.2–27.8 GHz and return loss of < -27 dB. In the second last step, the elliptical stub is loaded as in Ref. [33], which results in improved bandwidth as well as reduced return loss of the antenna. The antenna after this stage offers the least value of return loss around < -40 dB. In the final phase of design, a circular-shaped slot is etched into the elliptical patch to make the antenna operational at a wideband of 24.5–30.5 GHz. The design stages along with their impact on S_{11} are given in Fig. 4.

2.2. Results of single element

The $|S_{11}|$ parameter and gain of the suggested configuration are displayed in Fig. 5(a–b). The curves indicate that the antenna delivers a significant bandwidth (24.2–30 GHz) with a return loss of about -45 dB. With peak values of 9 dBi at 25.7 GHz and 28.5 GHz, the antenna also gives a high gain of >7.5 dBi in the operational region. Moreover, hardware measurements are also performed to validate the simulated results. It can be seen that software-generated and tested outcomes are quite similar. These outcomes prove that the design is the best candidate for IoT devices in future communication systems.

This suggested millimeter wave antenna's radiation pattern at the chosen frequencies of 26.5 GHz and 28 GHz is shown in Fig. 6 (a–b). It is clear that the antenna emits a wide side radiation pattern across both frequencies in the E-plane. The radiation pattern is slightly distorted in the H-plane due to multiple stub loadings and slot etching. The antenna radiation pattern is observed that it is not directional, which is due to the slot etched [34]. Moreover, the similarity between the simulated and measured patterns is also observed.

3. MIMO antenna design and results

3.1. Design of MIMO antenna

The same element is positioned orthogonally to the existing element in a two-port MIMO arrangement. A C-shaped parasitic component is positioned there to further the isolation at a distance of $S = 4.25$ mm between the two elements. The exact same material is used to construct the MIMO antenna as it is to create a single element. $M_X \times M_Y = 12$ mm $\times$ 20 mm is the MIMO antenna's entire dimension. Additionally, a model of the hardware is created to validate the output of the software. Fig. 7 represents the MIMO antenna structure and prototype.

Initially, a simple two-port MIMO antenna was engineered, which has a minimum mutual coupling of -17 dB and a maximum of -15 dB. After placing a C-shaped parasitic patch, the isolation of the antenna is refined. The resultant antenna offers mutual coupling with a maximum value of -22 dB and a minimum of -28 dB. The contrast between transmission coefficients to study the isolation of antennas with and without decoupling structures is given in Fig. 8.

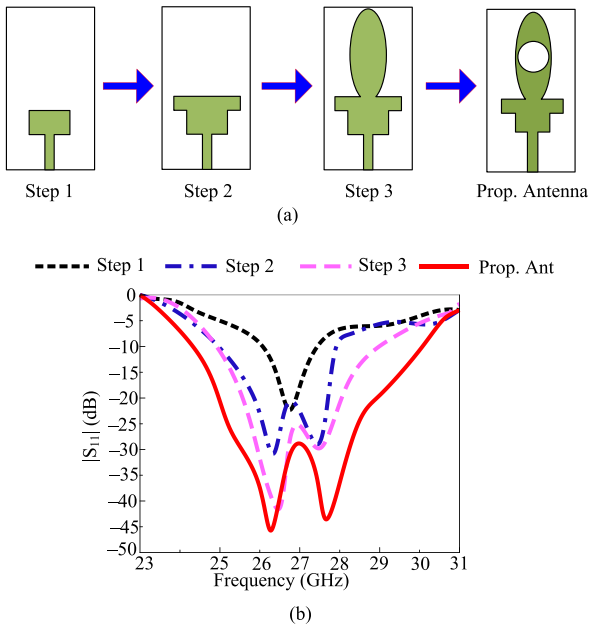

Fig. 4. Proposed work design evolution along with its impact on the S-parameter graph.

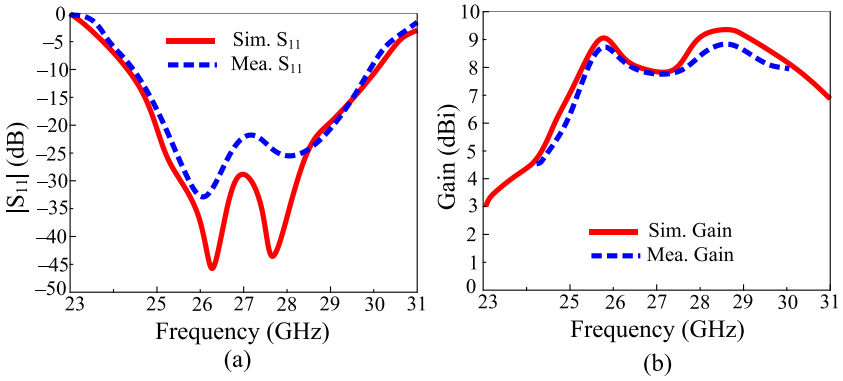

Fig. 5. Measured and simulated (a) S-parameter and (b) gain of proposed dual band antenna.

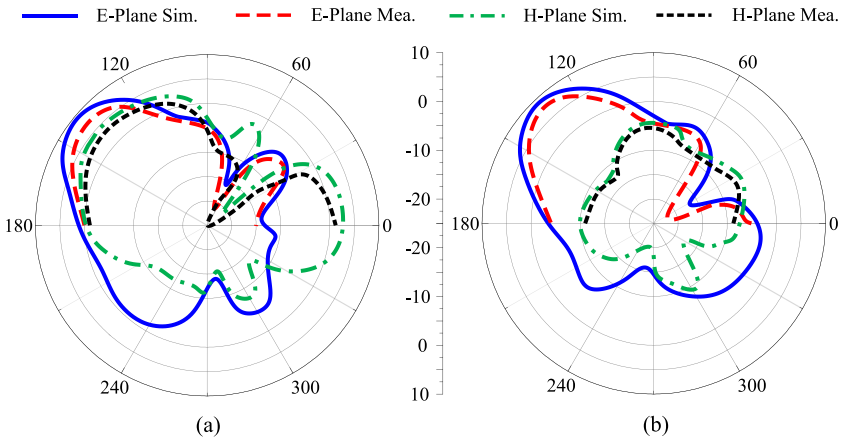

Fig. 6. Measured and simulated radiation pattern of unit element at (a) 26.5 GHz (b) 28 GHz.

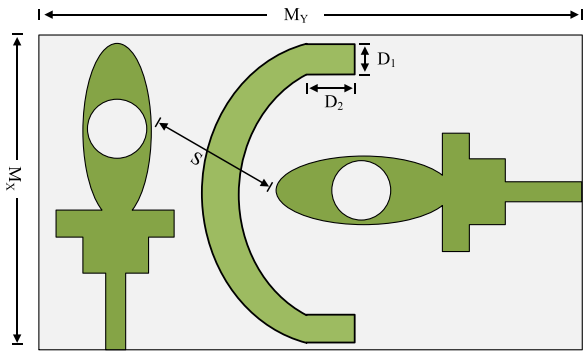

Fig. 7. Proposed MIMO antenna along with decoupling parasitic patch.

3.2. Hardware and measurements

The hardware model of the recommended two-port MIMO antenna for Internet of Things applications is shown in Fig. 9(a–b). To better understand the size of the antenna, it is kept together with a scale and a coin. The antenna is small and has a simplistic shape. The antenna is connected using an SMA connector. The VNA network analyzer is utilized for S-parameter analysis, and far-field measurement antennas are positioned in front of the horn antenna in the anechoic chamber.

The suggested work's reflection and transmission coefficients are displayed in Fig. 10(a–b). The findings show that the antenna has a wideband between 24 and 30.4 GHz with a minimum return loss of −43 dB. Exceptional transmission coefficient values are provided by the antenna, with a minimum value of −28 dB and a maximum value of −22 dB. These values are obtained after loading parasitic

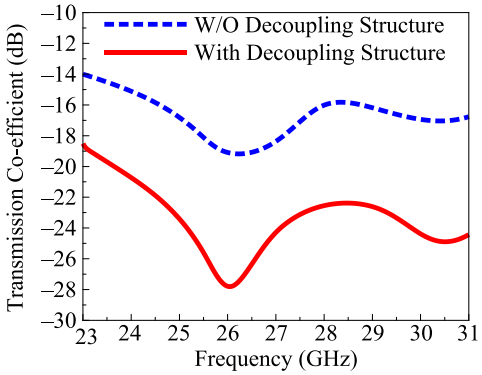

Fig. 8. Comparison of transmission co-efficient plot with and without parasitic element.

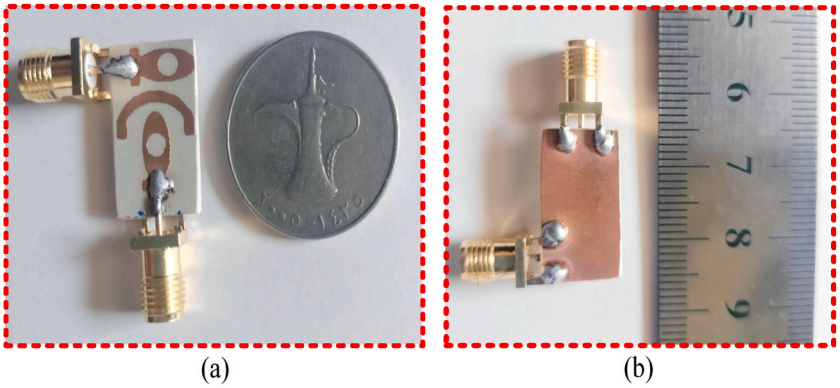

Fig. 9. Hardware model of the recommended antenna (a) front view (b) back view.

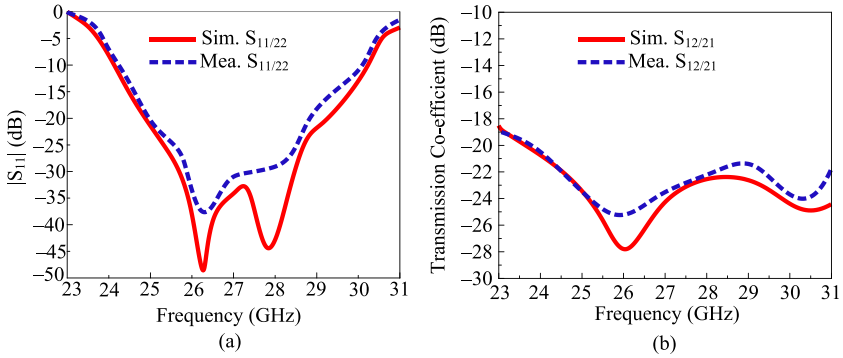

Fig. 10. Comparison of transmission S-parameters with and without parasitic element.

structures between MIMO elements. Moreover, the tested results are also inserted with software-generated results for better comparison. It can be noticed that the simulated and tested results are very similar, with little distortion that may occur due to measurement apparatus errors or human errors.

The planned antenna's radiation pattern for its specified frequencies of 26.5 GHz and 28.5 GHz is displayed in Fig. 11(a–b). The provided figure makes it clear that the most radiation that a MIMO antenna gives off happens on the broad side at both frequencies. The influence of antenna 2 on antenna 1 and vice versa causes the radiation pattern to be somewhat tilted, but generally, the antenna gives a table radiation pattern. For easier comprehension, the patterns are examined in the E and H planes. The measurement of distant fields is also carried out, and the outcomes sufficiently match those produced by the software.

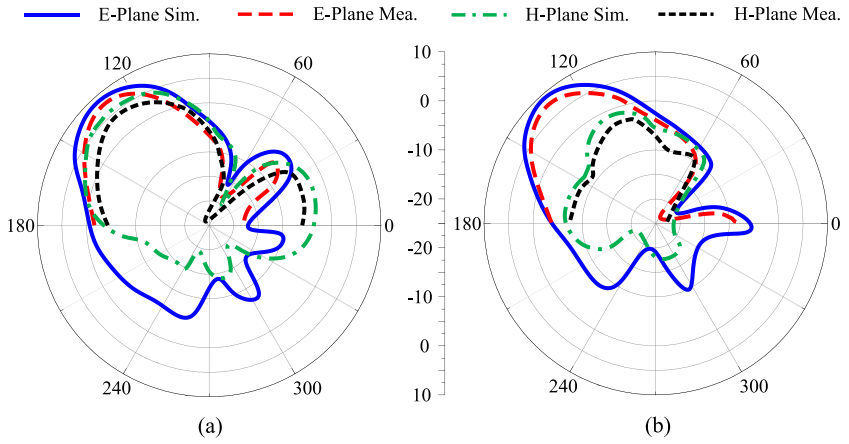

Fig. 11. Hardware tested and simulated radiation pattern of MIMO antenna at (a) 26.5 GHz and (b) 28.5 GHz.

3.3. MIMO performance parameters

Studying the MIMO antenna parameters is crucial and needed for future validation. In order to evaluate the effectiveness of the proposed antenna, a number of MIMO parameters in terms of ECC, CCL, DG, and MEG are researched and discussed. The antenna provides ECC within the permissible range, as can be seen in Fig. 12 (a) [35,36]. The operative band ECC of the antenna is 0.005. Additionally, ECC is researched to examine each component of MIMO antennas. Channel capacity loss (CCL), shown in Fig. 12 (b), is another metric. Ideally, the value of CCL should not be greater than 0.4 bits/s/Hz [37], where the suggested antenna offers CCL $<$0.3 bits/s/Hz.

Diversity gain (DG) is another important MIMO parameter that shows the power losses during transmission. Fig. 12 (c) shows that an antenna offers a diversity gain of around 9.99 dB and $>$9 dB at operational bandwidth. Ideally, the value of DG is 10 dB, while the suggested antenna offers a close value. The last MIMO parameter is mean effective gain (MEG), which is the study of the ratio between incident and received power. The acceptable value of MEG is between $-$3 and $-$10 dB, and the suggested antenna offers a value within the acceptable range as given in Fig. 12 (d).

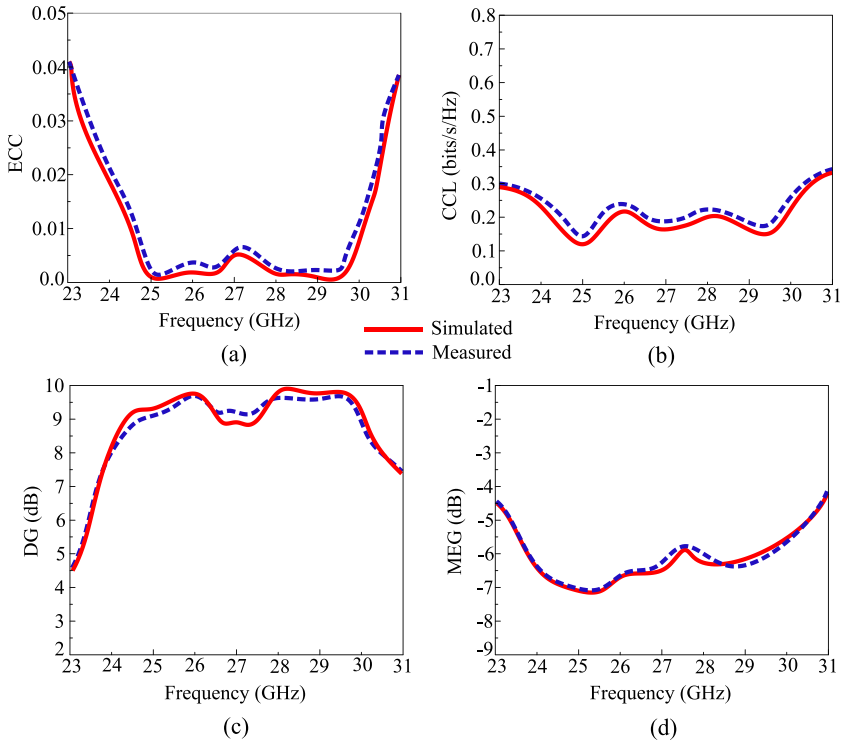

Fig. 12. (a) Envelop correlation coefficient (b) Channel capacity loss (c) diversity gain (d) mean effective gain of the suggested antenna.

3.4. Comparison with state-of-the-art

The distinction between the recommended MIMO antenna design and previously published models is shown in Table 1. Size, isolation improvement, bandwidth, and the technique used for isolation improvement are used to distinguish between recommended work and previously published work. In comparison to the other literary works, it can be said that the proposed work offers a compact size. Even if the approach described in Refs. [23,25] provides superior isolation, it lacks narrowband and is larger in size. As a result, it can be seen from the comparison table that the suggested work has improved performance, making it a good choice for mm-wave IoT devices.

4. Conclusion

This study proposes a compact, low-profile antenna with simple construction, aiming to provide wideband coverage, high gain, and a stable radiation pattern. The intention is to develop an antenna suitable for upcoming 5G and 6G devices. To enhance the antenna's performance, a two-port multiple-input multiple-output (MIMO) configuration is utilized to improve the data rate capabilities. However, it is found that the initial two-port MIMO antenna design does not exhibit satisfactory isolation between its elements. In order to address this issue, a C-shaped parasitic patch is introduced to refine the isolation characteristics of the antenna. As a result, the isolation is refined and enhanced from −18 dB to −28 dB, enhancing the performance of the MIMO antenna. The suggested MIMO antenna, integrated with the decoupling structure, provides wideband frequency coverage ranging from 24 GHz to 30.25 GHz, along with a high gain of 9.5 dBi. Additionally, various MIMO parameters are analyzed to assess the antenna's performance. The examination reveals that the antenna demonstrates an Error Correcting Code (ECC) value of approximately 0.005, a Cross-Correlation Level (CCL) below 0.3 bit/s/Hz, a Diversity Gain (DG) of around 9.99 dB, and a Mean Effective Gain (MEG) below −5.5 dB. To validate the proposed design, a hardware prototype of the antenna is constructed and tested, confirming the accuracy of the results obtained from software simulations. Furthermore, a comparison is made between the suggested antenna's performance and the findings reported in existing literature, highlighting the strengths of the recommended design. Based on the results and the comparison with previous work, it can be figured out that the suggested methodology is highly competitive and one of the most suitable choices for future Internet of Things (IoT) devices operating with wideband coverage and high gain requirements.

Author contribution statement

Wahaj Abbas Awan: Conceived and designed the experiments; Contributed reagents, materials, analysis tools or data; Wrote the paper.

Esraa Mousa Ali: Conceived and designed the experiments; Wrote the paper.

Mohammed S. Alzaidi; Dalia H. Elkamchouchi: Performed the experiments; Wrote the paper.

Fahad N Alsunaydih; Fahd Alsaleem; Khaled Alhassoon: Analyzed and interpreted the data; Contributed reagents, materials, analysis tools or data; Wrote the paper.

Data availability statement

Data included in article/supplementary material/referenced in article.

Funding

This work was supported by Princess Nourah bint Abdulrahman University Researchers Supporting Project number (PNURSP2023R238), Princess Nourah bint Abdulrahman University, Riyadh, Saudi Arabia.

Table 1
Presented design comparison with design published in the literature.

Ref	Size (mm × mm)	Isolation of simple design (dB)	Isolation refined (dB)	Gain (dB)	Operational Bandwidth (GHz)	Number of Antennas	The technique used to refine isolation
[24]	20 × 20	−16	−24	–	27.5–28.35	2	Metal strip
[25]	85 × 21	−22	−38	16.3	27–32	2	Meta surface
[26]	30 × 35	−15	−40	12	27.5–28.5	4	Parasitic Patch
[27]	30 × 43	−32	−45	10.2	24.55–26.5	4	Meta surface
[28]	25 × 15	−14	−41	6.3	26–30.5	2	DRA
[29]	48 × 31	–	−21	10	26–31	4	Parasitic Patch
[30]	26 × 14.5	−19	−22	4.5	27–29	2	Meta surface
[31]	20 × 40	−18	−28	9	27.5–28.5	4	Meta surface
Prop.	12 × 20	−18	−29	9.25	24–30.25	2	Parasitic Patch

Additional information

No additional information is available for this paper.

Declaration of competing interest

We, all authors listed as "*Wahaj Abbas Awan, Esraa Mousa Ali, Mohammed S. Alzaidi, Dalia H. Elkamchouchi, Fahad N Alsunaydih, Fahd Alsaleem, Khaled Alhassoon*", are submitting our recent research work in its revised version entitled "*Enhancing Isolation Performance of Tilted Beam MIMO Antenna for Short-Range Millimeter Wave Applications*" to *Heliyon* for its consideration for possible publications after evaluation by your editorial boards and reviewers.

So, all of authors have read the paper and are agree for its submission to Heliyon and we do not have any Conflict of Interest.

Acknowledgments

Princess Nourah bint Abdulrahman University Researchers Supporting Project number (PNURSP2023R238), Princess Nourah bint Abdulrahman University, Riyadh, Saudi Arabia. Moreover, researchers would like to thank the Deanship of Scientific Research, Qassim University, for funding the publication of this project.

References

[1] M. Hussain, W.A. Awan, M.S. Alzaidi, N. Hussain, E.M. Ali, F. Falcone, Metamaterials and their application in the performance enhancement of reconfigurable antennas: a review, Micromachines 14 (2023) 349.
[2] H. Zahra, M. Hussain, S. Shrestha, M. Asadnia, S.M. Abbas, S. Mukhopadhyay, Printed planar antenna for 28GHz 5G millimeter-wave applications, in: International Symposium on Antennas and Propagation and USNC-URSI Radio Science Meeting, AP-S/URSI, 2022, pp. 53–54.
[3] W.A. Awan, A. Zaidi, A. Baghdad, Patch antenna with improved performance using DGS for 28GHz applications, in: International Conference on Wireless Technologies, Embedded and Intelligent Systems, WITS, 2019, pp. 1–4.
[4] N. Hussain, W.A. Awan, W. Ali, S.I. Naqvi, A. Zaidi, T.T. Le, Compact wideband patch antenna and its MIMO configuration for 28 GHz applications, AEU-International Journal of Electronics and Communications 132 (2021), 153612.
[5] M. Hussain, A. Mazher, E. Chaudary, B. Hussain, M. Alibakhshikenari, F. Falcone, E. Limiti, Compact dual-band antenna with high gain and simple geometry for 5G cellular communication operating at 28 GHz and 44 GHz, in: XXXIVth General Assembly and Scientific Symposium of the International Union of Radio Science, URSI GASS, 2021, pp. 1–4.
[6] M. Hussain, E. Mousa Ali, S.M.R. Jarchavi, A. Zaidi, A.I. Najam, A.A. Alotaibi, A. Althobaiti, S.S.M. Ghoneim, Design and characterization of compact broadband antenna and its MIMO configuration for 28 GHz 5G applications, Electronics 11 (2022) 523.
[7] M. Hussain, W.A. Awan, E.M. Ali, M.S. Alzaidi, M. Alsharef, D.H. Elkamchouchi, A. Alzahrani, M. Fathy Abo Sree, Isolation improvement of parasitic element-loaded dual-band MIMO antenna for mm-wave applications, Micromachines 13 (2022) 1918.
[8] J. Zhang, X. Ge, Q. Li, M. Guizani, Y. Zhang, 5G millimeter-wave antenna array: design and challenges, IEEE Wireless Commun. 24 (2) (2016) 106–112.
[9] A. Patel, A. Vala, A. Desai, I. Elfergani, H. Mewada, K. Mahant, C. Zebiri, D. Chauhan, J. Rodriguez, Inverted-L shaped wideband MIMO antenna for millimeter-wave 5G applications, Electronics 11 (2022) 1387.
[10] M.I. Khan, S. Khan, S.H. Kiani, N. Ojaroudi Parchin, K. Mahmood, U. Rafique, M.M. Qadir, A Compact mmWave MIMO antenna for future wireless networks, Electronics 11 (2022) 2450.
[11] D.T.T. Tu, N.G. Thang, N.T. Ngoc, N.T.B. Phuong, V. Van Yem, 28/38 GHz dual-band MIMO antenna with low mutual coupling using novel round patch EBG cell for 5G applications, International Conference on Advanced Technologies for Communications (ATC) (2017) 64–69.
[12] S.A. Hussain, F. Taher, M.S. Alzaidi, I. Hussain, R.M. Ghoniem, M.F.A. Sree, A. Wideband Lalbakhsh, high-gain, and compact four-port MIMO antenna for future 5G devices operating over Ka-band spectrum, Appl. Sci. 13 (2023) 4380.
[13] A. Desai, C.D. Bui, J. Patel, T. Upadhyaya, G. Byun, T.K. Nguyen, Compact wideband four element optically transparent MIMO antenna for mm-wave 5G applications, IEEE Access 8 (2020) 194206–194217.
[14] A.A.R. Saad, H.A. Mohamed, Printed millimeter-wave MIMO-based slot antenna arrays for 5G networks, AEU-International Journal of Electronics and Communications 99 (2019) 59–69.
[15] H.M. Marzouk, M.I. Ahmed, A.A. Shaalan, A novel dual-band 28/38 GHz AFSL MIMO antenna for 5G smartphone applications, J. Phys. Conf. 1447 (1) (2020), 012025.
[16] I. Elfergani, J. Rodriguez, A. Iqbal, M. Sajedin, C. Zebiri, R.A. AbdAlhameed, Compact millimeter-wave MIMO antenna for 5G applications, in: 2020 14th European Conference on Antennas and Propagation, EuCAP), 2020, pp. 1–5.
[17] A.T. Alreshaid, R. Hussain, S.K. Podilchak, M.S. Sharawi, A Dual-Element MIMO Antenna System with a Mm-Wave Antenna Array, 10th European conference on antennas and propagation (EuCAP), 2016, pp. 1–4.
[18] H. Xing, X. Wang, Z. Gao, X. An, H.X. Zheng, M. Wang, E. Li, Efficient isolation of a MIMO antenna using defected ground structure, Electronics 9 (2020) 1265.
[19] M. Abdullah, S.H. Kiani, A. Iqbal, Eight element multiple-input multiple-output (MIMO) antenna for 5G mobile applications, IEEE Access 7 (2019) 134488–134495.
[20] A. Altaf, A. Iqbal, A. Smida, J. Smida, A.A. Althuwayb, S. Hassan Kiani, M. Alibakhshikenari, F. Falcone, E. Limiti, Isolation improvement in UWB-MIMO antenna system using slotted stub, Electronics 9 (2020) 1582.
[21] S. Rajkumar, A. Anto Amala, K.T. Selvan, Isolation improvement of UWB MIMO antenna utilising molecule fractal structure, Electron. Lett. 55 (10) (2019) 576–579.
[22] B. Xiao, H. Wong, D. Wu, K.L. Yeung, Design of small multiband full-screen smartwatch antenna for IoT applications, IEEE Internet Things J. 8 (24) (2021) 17724–17733, https://doi.org/10.1109/JIOT.2021.3082535, 15 Dec.15.
[23] P. Kumar, S. Urooj, A. Malibari, Design and implementation of quad-element super-wideband MIMO antenna for IoT applications, IEEE Access 8 (2020) 226697–226704, https://doi.org/10.1109/ACCESS.2020.3045534.
[24] Y. Zhang, J.Y. Deng, M.J. Li, D. Sun, L.X. Guo, A MIMO dielectric resonator antenna with improved isolation for 5G mm-wave applications, IEEE Antenn. Wireless Propag. Lett. 18 (4) (2019) 747–751.
[25] S. Gupta, Z. Briqech, A.R. Sebak, T.A. Denidni, Mutual-coupling reduction using metasurface corrugations for 28 GHz MIMO applications, IEEE Antenn. Wireless Propag. Lett. 16 (2017) 2763–2766.
[26] M. Bilal, S.I. Naqvi, N. Hussain, Y. Amin, N. Kim, High-isolation MIMO antenna for 5G millimeter-wave communication systems, Electronics 11 (2022) 962.
[27] S. Tariq, S.I. Naqvi, N. Hussain, Y. Amin, A metasurface-based MIMO antenna for 5G millimeter-wave applications, IEEE Access 9 (2021) 51805–51817.
[28] M.D. Alanazi, S.K. Khamas, A compact dual band MIMO dielectric resonator antenna with improved performance for mm-wave applications, Sensors 22 (2022) 5056.

[29] Z. Wani, M.P. begaonkar, S.K. Koul, A 28-GHz antenna for 5G MIMO applications, Progress In Electromagnetics Research Letters 78 (2018) 73–79.
[30] B.A. Esmail, S. Koziel, High isolation metamaterial-based dual-band MIMO antenna for 5G millimeter-wave applications, AEU-International Journal of Electronics and Communications 158 (2023), 154470.
[31] N. Murthy, Improved isolation metamaterial inspired mm-Wave MIMO dielectric resonator antenna for 5G application, Prog. Electromagn. Res. C 100 (2020) 247–261.
[32] C.A. Balanis, Antenna Theory: Analysis and Design, John wiley & sons, 2016.
[33] I.A. Awan, M. Hussain, S.N.R. Rizvi, M. Alibakhshikenari, F. Falcone, E. Limiti, Single patch fractal-shaped antenna with small footprint area and high radiation properties for wide operation over 5G region, in: 46th International Conference on Infrared, Millimeter and Terahertz Waves, IRMMW-THz, Chengdu, China, 2021, pp. 1–2.
[34] R. Hussain, M. Abou-Khousa, N. Iqbal, A. Algarni, S.I. Alhuwaimel, A. Zerguine, M.S. Sharawi, A multiband shared aperture MIMO antenna for millimeter-wave and sub-6GHz 5G applications, Sensors 22 (5) (2022) 1808.
[35] A. Quddus, R. Saleem, T. Shabbir, S.U. Rehman, M.F. Shafique, Dual port UWB-MIMO antenna with ring decoupling structure, in: Progress in Electromagnetic Research Symposium, PIERS, Shanghai, China, 2016, pp. 116–119.
[36] W. Wang, et al., Wideband gain enhancement of MIMO antenna and its application in FMCW radar sensor integrated with CMOS-based transceiver chip for human respiratory monitoring, IEEE Trans. Antenn. Propag. 71 (1) (Jan. 2023) 318–329, https://doi.org/10.1109/TAP.2022.3222802.
[37] W. Wang, Y. Zheng, Wideband gain enhancement of high-isolation fabry–pérot antenna array with tandem circular parasitic patches and radial gradient PRS, IEEE Trans. Antenn. Propag. 69 (11) (Nov. 2021) 7959–7964, https://doi.org/10.1109/TAP.2021.3083781.